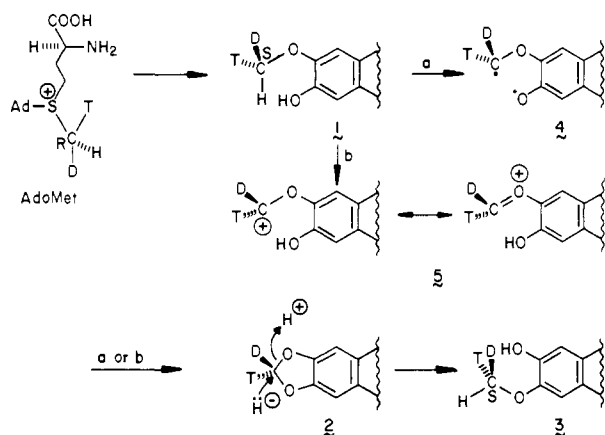


Scheme III



The formation of the 2-*O*-methyl group of **3** was studied *in vivo* in callus cultures of *Berberis koetianeana*, because the enzyme catalyzing the opening of the methylenedioxy bridge has not yet been isolated. To this end, (1*S*,methyl-*S*)- and (1*S*,methyl-*R*)-[6-*O*-methyl-²H,³H]reticuline were synthesized from the above samples of chiral AdoMet with porcine liver catechol *O*-methyltransferase (COMT) (Sigma) (Sigma) to transfer the methyl group with inversion of configuration.¹⁰ The two substrates were purified to remove any traces of the 7-*O*-methyl isomer and fed to the callus cultures. The resulting samples of **3**, purified to remove traces of other alkaloids, particularly **1**, were again degraded as shown in Scheme II. *F* values of 55.4 and 44.2 for the acetic acids obtained indicated 19% ee *S* and 20% ee *R* configuration, respectively, for the methyl groups of the two samples of **3**. Hence the conversion sequence **1** → **2** → **3** has produced a methyl group in **3** of the same configuration as that in **1**.

The abstraction of a hydrogen from the 3-*O*-methyl group of **1** proceeds without an isotope effect³ and will thus produce equal amounts of methylene groups in **2** containing ³H plus ²H and ³H plus ¹H. In the subsequent opening of the methylenedioxy bridge, the former will give chiral and the latter achiral methyl groups in **3**. If both steps were completely stereospecific, the enantiomeric purities of the methyl groups in the two samples of **3** would be 44% and 43% ee, respectively.²⁴ The significantly lower observed values indicate that at least one of the two steps must be accompanied by substantial racemization. The stereochemical results are consistent with, although do not prove, a mechanism as shown in Scheme III. Abstraction of H[•] from the methyl group and the adjacent OH gives diradical **4**, which collapses with C–O bond formation on the same side on which H[•] has been removed (path a). Competing rotation and inversion of the methylene radical accounts for the observed racemization. An equally plausible alternative is ring closure and racemization via the cationic intermediate **5** (path b). Opening of the methylenedioxy bridge occurs by attack of H[−] on a trajectory opposite the CH₂–O-3 bond, possibly assisted by conjugation to the positively charged nitrogen of **2**,⁷ replacing O-3 by H with inversion of configuration.

(19) However, several examples of methyl transfer with net retention of configuration have recently been uncovered,^{20–23} including two cases involving transfer of the methyl group of methionine.^{22,23} These are thought to represent two-step processes.

(20) Zydowsky, T. M.; Courtney, L. F.; Frasca, V.; Kobayashi, K.; Shimizu, H.; Yuen, L.-D.; Matthews, R. G.; Benkovic, S. J.; Floss, H. G. *J. Am. Chem. Soc.* **1986**, *108*, 3152–3153.

(21) Lebertz, H.; Simon, H.; Courtney, L. F.; Benkovic, S. J.; Zydowsky, L. D.; Lee, K.; Floss, H. G. *J. Am. Chem. Soc.* **1987**, *109*, 3173–3174.

(22) Houck, D. R.; Kobayashi, K.; Williamson, J. M.; Floss, H. G. *J. Am. Chem. Soc.* **1986**, *108*, 5365–5366.

(23) A methionine-dependent methylation in the biosynthesis of the antibiotic thiostrepton also proceeds with net retention of methyl group configuration (Yuen, L.-D.; Floss, H. G., unpublished results).

(24) This prediction makes the reasonable assumption that COMT methylates *O*-6 with the same degree of stereospecificity as the plant enzyme. The slightly lower *F* values reported¹⁰ almost certainly are due to the stereochemically less stringent degradation procedure used in the earlier work.

Acknowledgment. We thank Kyungok Lee for carrying out the chirality analyses of the acetate samples and Dr. T. M. Zydowsky for the synthesis of the chiral acetic acid used in the preparation of AdoMet. Financial support of this work by the Deutsche Forschungsgemeinschaft (SFB 145), the Fonds der Chemischen Industrie, and the National Institutes of Health (Grant GM-32333) is gratefully acknowledged.

Observation of Medium Chain Length Polymethylene Biradicals in Liquid Solutions by Time Resolved EPR Spectroscopy¹

Gerhard L. Closs*^{†‡} and Malcolm D. E. Forbes[†]

Department of Chemistry, The University of Chicago
Chicago, Illinois 60637
Chemistry Division, Argonne National Laboratory
Argonne, Illinois 60439

Received April 6, 1987

In recent years much effort has been expended on the detection of unstable biradicals by physical methods.² Because of its superior time resolution, optically detected laser flash photolysis has been the method of choice for obtaining kinetic information. However, the broad solution spectra have little structural content, and the method fails entirely when the biradical has no useful absorption band. Consequently, no spectroscopic measurements of any kind have been reported on the fundamental polymethylene chain biradicals.³ In this communication we report the first EPR spectra of localized polymethylene biradicals obtained in liquid solution under conditions where they undergo normal fast reactions.

The biradicals were generated in hydrocarbon solvents by photolysis with an excimer laser operating at 308 nm from cyclic α,ω -methylated cycloalkanones **1** by photochemical Norrish type I cleavage followed by fast thermal decarbonylation as shown in Scheme I. The reactions were run in the optical transmission cavity of an X-band EPR spectrometer modified for direct detection and boxcar averaging, operating with a gate of 100 ns at temperatures ranging from −10 to 60 °C with use of a flow system to prevent sample depletion.⁴

Figure 1A shows a series of spectra obtained from the photolysis of tetramethylcycloalkanones (**1**, R₁ = R₂ = CH₃; *n* = 10, 9, 8) observed at 0.25 and 1.0 μ s. It is clear from inspection that the two spectra obtained from the cyclododecanone (*n* = 9) and measured at different delay times are caused by two different carriers. They are assigned to the acyl-alkyl biradical **2** at early times, subsequently evolving into the dialkyl biradical **3**. Although not shown, the other ketones give similar spectra at early times. Also, with decreasing chain length, the spectra take on a net emissive character.

The model used to interpret the strongly polarized spectra and their time evolution is shown schematically in Figure 2 and is essentially identical with the quantitative model developed recently for radical pairs in micelles.⁵ Nonadiabatic bond breaking in

[†] The University of Chicago.

[‡] Argonne National Laboratory.

(1) Work supported by NSF Grant CHE-8520326.

(2) (a) Scaiano, J. C. *Acc. Chem. Res.* **1982**, *15*, 252. (b) Scaiano, J. C. *Tetrahedron* **1982**, *38*, 819. (c) Zimmt, M. B.; Doubleday, C.; Turro, N. J. *J. Am. Chem. Soc.* **1986**, *108*, 3618.

(3) Notable exceptions are the EPR measurements on matrix isolated cycloalkanediyls: (a) Buchwalter, S. L.; Closs, G. L. *J. Am. Chem. Soc.* **1975**, *97*, 3857; **1979**, *101*, 4688. (b) Jain, J.; Snyder, G. J.; Dougherty, D. A. *J. Am. Chem. Soc.* **1984**, *106*, 7294.

(4) A more detailed description of the apparatus is given in ref 5.

(5) (a) Closs, G. L.; Forbes, M. D. E.; Norris, J. R. *J. Phys. Chem.* **1987**, *91*, 3592. (b) Buckley, C. D.; Hunter, D. A.; Hore, P. J.; McLauchlan, K. A. *Chem. Phys. Lett.* **1987**, *135*(3), 307.

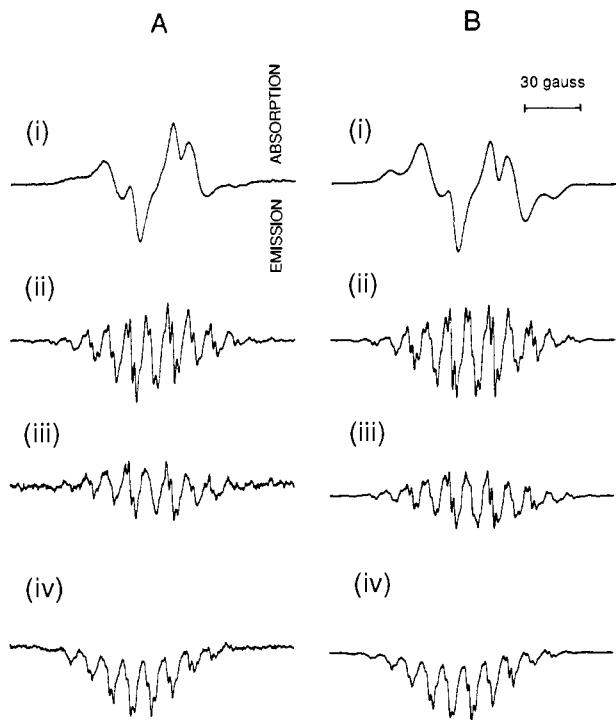
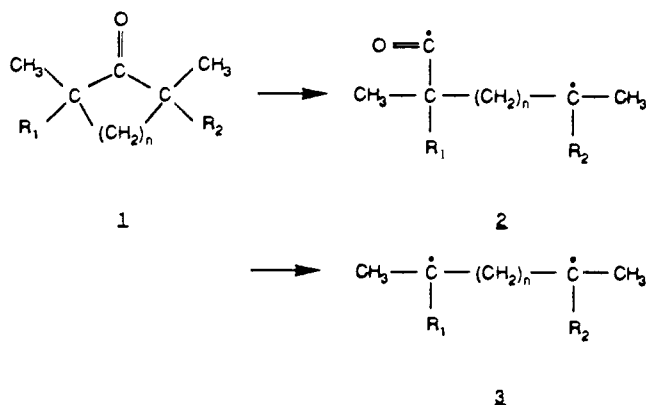


Figure 1. (A) EPR spectra of the following: (i) **2** ($R_1 = R_2 = \text{CH}_3$, $n = 9$) at $0.25 \mu\text{s}$; (ii) **3** ($R_1 = R_2 = \text{CH}_3$, $n = 9$) at $1 \mu\text{s}$; (iii) **3** ($R_1 = R_2 = \text{CH}_3$, $n = 10$) at $1 \mu\text{s}$; (iv) **3** ($R_1 = R_2 = \text{CH}_3$, $n = 8$) at $1 \mu\text{s}$. (B) Simulations with constants common to all four spectra: hf coupling $\text{CH}_3 = 62.2 \text{ MHz}$, $\text{CH}_2 = 49.8 \text{ MHz}$; $g(\text{alkyl}) = 2.0026$, $g(\text{acyl}) = 2.0008$; $k_{T^0} = k_r \lambda^0$, $k_{S'} = k_r(1 - \lambda^0)$, $k_r = 10^{10} \text{ s}^{-1}$; $k_{T^+} = k_p \lambda^+$, $k_p = 10^9 \text{ s}^{-1}$. Specifically for the following: (i) $-J = 98 \text{ MHz}$, $k_{T^-} = k_m \lambda^-$, $k_m = 1.2 \times 10^9 \text{ s}^{-1}$, linewidth (LW) = 8 G ; 7b (ii) $-J = 390 \text{ MHz}$, $k_m = 1.2 \times 10^9 \text{ s}^{-1}$, LW = 2 G ; (iii) $-J = 210 \text{ MHz}$, $k_m = 1.2 \times 10^9 \text{ s}^{-1}$, LW = 2 G ; (iv) $-J = 1120 \text{ MHz}$, $k_m = 3.6 \times 10^9 \text{ s}^{-1}$. λ^{\pm} are on the order of 10^{-3} – 10^{-6} .

Scheme 1



the triplet ketone yields equally populated, nonstationary triplet spin states of the biradical, T^- , T^0 , T^+ , with singlet state, S , being empty. Hyperfine induced mixing develops the wave function, admixing fractions of singlet character into the triplet functions, and distributes the populations accordingly. With a small exchange coupling J , the mixing is mostly between S and T^0 , yielding the mixed states S' and $T^{0'}$, while T^+ and T^- remain relatively pure. But if J is negative and approaches the Zeeman splitting ($g\beta B_0$), T^- will acquire substantial singlet character too. It should be noted that J depends on the conformation of the chain, and what is observed is a weighted average over all conformations.

Next, the model assumes that the rates for biradical cyclization and disproportionation are proportional to the singlet character of the states (λ^+ , λ^0 , λ^-), on the order of 10^{-3} – 10^{-6} depending on the nuclear substates, requiring that the exit rates are weighted accordingly. For a small and negative J the disappearance of the four electronic states will obey the order $S' > T^{0'} > T^- > T^+$. Application of this model to the systems studied predicts spectra

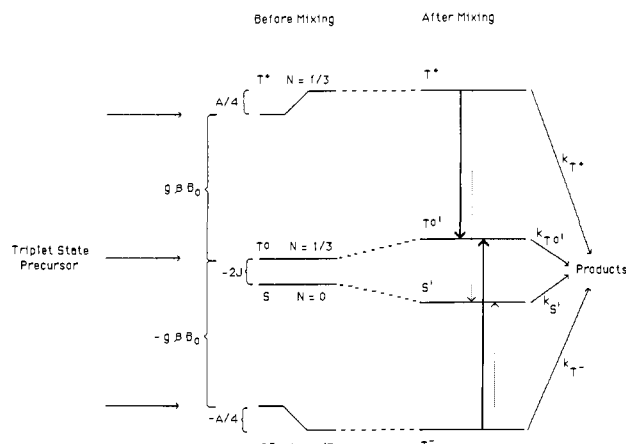


Figure 2. Schematic energy level diagram for a biradical with one hyperfine interaction (A) being populated nonadiabatically from a triplet precursor and forming products with the rates corresponding to the constants shown. The transitions indicated by heavy arrows correspond to the ones observed. The dotted arrows indicate transitions forbidden when $|J| \gg \text{hf coupling}$.

with equal emission and absorption for the longer chains, turning into net emission with decreasing length.⁶

The results of the simulations with parameters stated are given in Figure 1B. The magnetic parameters used for the simulation of the two observed biradicals, **2** and **3**, are taken from the corresponding monoradicals reported in the literature,⁷ and the exchange interaction, J , was adjusted for the best fit as were the kinetic exit rate constants.⁸ Besides the excellent agreement of the simulations with experiment, several other factors serve as compelling evidence for the assignment of the spectra. The slight asymmetry of line positions and intensities in the early spectrum can only arise from g factor differences on the biradical centers. At later times ($\sim 1 \mu\text{s}$ at 30°C) the spectra become symmetric, consistent with a change to a dialkyl biradical. The major spacings apparent in the dialkyl spectra are approximately one half of those observed for a corresponding monoradical as predicted by theory.⁹ Below room temperature (-6°C) the acyl type spectrum **2** persists for longer times ($\sim 1 \mu\text{s}$) while at higher temperature (50°C) the spectrum attributed to **3** appears almost from the beginning.¹⁰

So far, we have observed tertiary and secondary biradicals ($R_1 = R_2 = \text{CH}_3$; $R_1 = \text{CH}_3$, $R_2 = \text{H}$; $R_1 = R_2 = \text{H}$) of type **2** ranging from $n = 4$ – 13 and of type **3** from $n = 5$ – 13 with the lower members being all emissive ($|2J| \approx g\beta B_0$) and the higher ones of comparable emissive and absorptive character ($|2J| \ll g\beta B_0$). Observation of the less alkylated biradicals requires elevated temperature to speed up the decarbonylation. Limitations at the lower end is a J too large to allow effective triplet-singlet mixing. The higher end has not yet been explored.

Perhaps the most remarkable finding is the long lifetime of the dialkyl radicals ($> 1 \mu\text{s}$), although in view of previous work this

(6) This is in strict analogy to the emissive NMR spectra resulting from the products of the biradicals: Closs, G. L.; Miller, R. J.; Redwine, O. D. *Acc. Chem. Res.* **1985**, *18*, 196. Closs, G. L.; Redwine, O. D. *J. Am. Chem. Soc.* **1985**, *107*, 4543, 6131.

(7) (a) The 2-methyl-2-pentyl radical has been chosen as the model for the hyperfine coupling constants: Ohno, N.; Kito, N.; Ohnishi, Y. *Bull. Chem. Soc. Jpn.* **1971**, *44*, 470. (b) The g factor and line width of the acyl part of the biradical was set equal to that of the pivaloyl radical Schuh, H.; Hamilton, E. J., Jr.; Paul, H.; Fischer, H. *Helv. Chim. Acta* **1974**, *57*, 2011.

(8) The values for J , quoted in the legend of Figure 1 should be considered good to $\approx 20\%$. Outside of this limit noticeable discrepancies occur between simulations and experiment. Of course, the values are weighted averages over all conformers. The exit rate constants were adjusted to give a good fit, but the spectra are not sensitive to all of them. Therefore we attach not much meaning to them at this time.

(9) Reitz, D. C.; Weissman, S. I. *J. Chem. Phys.* **1960**, *33*, 700.

(10) The lifetimes reported for alkyl-acyl biradicals of type **2** are normally below $100 \text{ ns}^{2,6}$ while our earliest spectra are taken at 250 ns . This implies that we are observing only a very small fraction of the biradicals generated or that the biradical decay is not strictly exponential with a slower decaying tail fraction.

is not entirely unexpected.¹¹ The absence of any group with elements heavier than carbon reduces intersystem crossing by spin orbit coupling to a minimum making hyperfine induced mixing and spin lattice relaxation the major pathways. Analysis of the decay kinetics of the biradical signals requires the knowledge of the spin lattice relaxation times (T_1), and most likely the lifetimes of the biradicals are even longer than the decay constants of the signals. A detailed analysis is in progress.

Registry No. 1 ($n = 10$; $R_1 = R_2 = \text{CH}_3$), 110015-80-0; **1** ($n = 9$; $R_1 = R_2 = \text{CH}_3$), 60010-87-9; **1** ($n = 8$; $R_1 = R_2 = \text{CH}_3$), 110015-81-1; **2** ($n = 10$; $R_1 = R_2 = \text{CH}_3$), 110015-82-2; **2** ($n = 9$; $R_1 = R_2 = \text{CH}_3$), 110015-83-3; **2** ($n = 8$; $R_1 = R_2 = \text{CH}_3$), 110015-84-4; **3** ($n = 10$; $R_1 = R_2 = \text{CH}_3$), 110015-85-5; **3** ($n = 9$; $R_1 = R_2 = \text{CH}_3$), 110015-86-6; **3** ($n = 8$; $R_1 = R_2 = \text{CH}_3$), 110015-87-7.

(11) Zimmt, M. B.; Doubleday, C.; Gould, I. R.; Turro, N. J. *J. Am. Chem. Soc.* **1985**, *107*, 6724.

Total Synthesis of (\pm)-Atractyligenin

Ashok K. Singh, Raman K. Bakshi, and E. J. Corey*

Department of Chemistry, Harvard University
Cambridge, Massachusetts 02138

Received June 2, 1987

The thistle *Atractylis gummifera*, known since ancient times for its deadly toxicity, produces two poisonous principles which are derivatives of the diterpenoid atractyligenin (**1**).¹ These substances, atractyloside (**2**) and 4-carboxyatractyloside, function by blocking the transport of adenosine diphosphate (ADP) into mitochondria, thereby decreasing ATP production.¹⁻³ Atractylosides also occur in the coffee plants *Coffea arabica* and *Coffea robusta* and are consumed in non-negligible amounts by coffee drinkers.^{4,5} Our awareness of the anomalous situation in which a known toxin is unknowingly ingested by a large and metabolically variable human population and previous work on the ATP translocation inhibitor³ bongkreic acid⁶ aroused our interest in the synthesis and biochemistry of atractyligenin and its glycosides. The successful achievement of total synthesis of (\pm)-**1**⁷ is reported herein. A novel approach to the construction of the ring system developed for this problem has also been applied recently to the total synthesis of cafestol.⁸

o-Tolyethanol (formed in 97% yield by lithium aluminum hydride reduction in ether of *o*-tolylacetic acid) was reduced with excess lithium in tetrahydrofuran (THF)-ammonia-*tert*-amyl alcohol (1:1:1)⁹ at -45°C for 5 h to give the Birch product **3** (89%)

(1) For an outstanding treatise on atractylosides and atractyligenin; see: *Atractyloside: Chemistry, Biochemistry, and Toxicology*; Santi, R.; Luciani, S., Eds.; Piccin Medical Books: Padova, Italy, 1978.

(2) Klingenberg, M. in ref 1, pp 69-107.

(3) Klingenberg, M. *Trends Biochem. Sci.* **1979**, *4*, 249-252.

(4) See: Richler, H.; Spittler, G. *Chem. Ber.* **1978**, *111*, 3506-3509, and references cited therein for the occurrence of atractyligenin and its glycosides in human urine as a consequence of absorption from ingested coffee.

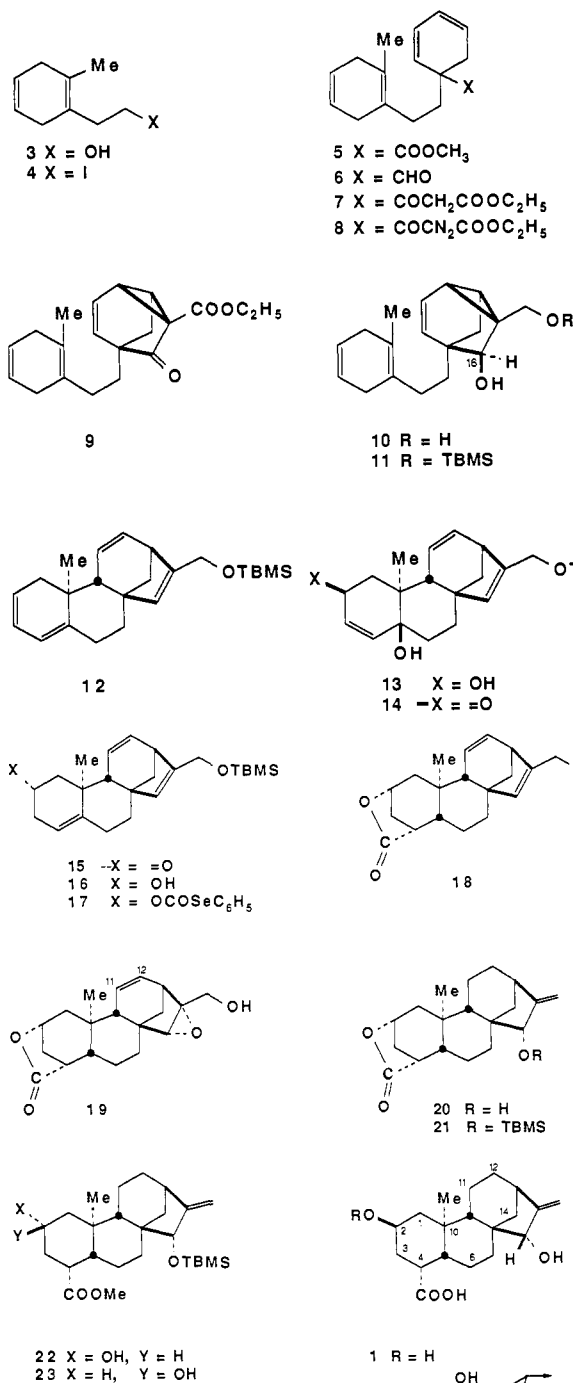
(5) An excellent summary of the literature on potential harmful effects of dietary atractylosides from coffee which has been provided by Pegel (Pegel, K. H. *Chem. Eng. News* **1981** (July 20) p 4) seems to have been largely ignored.

(6) Corey, E. J.; Tramontano, A. *J. Am. Chem. Soc.* **1984**, *106*, 462-463.

(7) For structure determination and chemistry of atractyligenin, see: (a) Piozzi, F.; Quilico, A.; Mondelli, R.; Ajello, T.; Sprio, V.; Malera, A. *Tetrahedron* **1966**, Suppl. 8, Part II, 515-529. (b) Piozzi, F., Quilico, A.; Fuganti, C.; Ajello, T.; Sprio, V. *Gazzetta Chem. Ital.* **1967**, *97*, 935-954. (c) Piozzi, F. in ref. 1, pp 13-32.

(8) Corey, E. J.; Wess, G.; Xiang, Y. B.; Singh, A. K. *J. Am. Chem. Soc.* **1987**, *109*, 4717-4718.

(9) Corey, E. J.; Katzanellenbogen, J. K.; Gilman, N. W.; Roman, S.; Erickson, B. W. *J. Am. Chem. Soc.* **1968**, *90*, 5618-5620.



which by treatment with 3 equiv each of triphenylphosphine, imidazole, and iodine in ether-acetonitrile (3:1) at 25°C for 30 min produced iodide **4** (93%). Methyl cyclohexa-1,3-diene-5-carboxylate¹⁰ was deprotonated (1.1 equiv of lithium diisopropylamide (LDA) in THF at -78°C for 1 h) and alkylated with iodide **4** (1.1 equiv) in the presence of 1 equiv of hexamethylphosphoric triamide at -78°C for 5 h and -78°C to -20°C for 9 h to afford bicyclic ester **5** (82%). Appendage elaboration to form the β -keto ester **7** was accomplished by the following sequence: (1) reduction by 5 equiv of diisobutylaluminum hydride in methylene chloride at -78°C for 2.5 h to give the corresponding primary alcohol (90%); (2) Swern oxidation with 1.2 equiv of oxalyl chloride, 2.6 equiv of dimethyl sulfoxide, and 5.5 equiv of

(10) Hoare, J. H.; Policastro, P. O.; Berchtold, G. A. *J. Am. Chem. Soc.* **1983**, *105*, 6264-6267.